Grain Boundary Misorientation Effects on Creep and Cracking in Ni-Based Alloys

Gary S. Was, Visit Thaveeprungsriporn, and Douglas C. Crawford

The effect of altered grain boundary character distributions on the creep and cracking behavior of polycrystalline Ni-16Cr-9Fe at 360°C was studied by comparing the creep and intergranular cracking behavior of solution-annealed material containing mostly high-angle boundaries to material that was thermomechanically processed to enhance the proportion of coincident-site lattice boundaries. In parallel with mechanical testing, the modification of dislocation structures in the grain boundary resulting from reactions with run-in lattice dislocations was studied using transmission electron microscopy. Observations were concerned with the ability of grain boundaries to act as sinks for lattice dislocations in which the kinetics depend on the grain-boundary structure. A mechanism based on dislocation annihilation was proposed to account for the observed effect of the coincident-site lattice boundaries on creep.

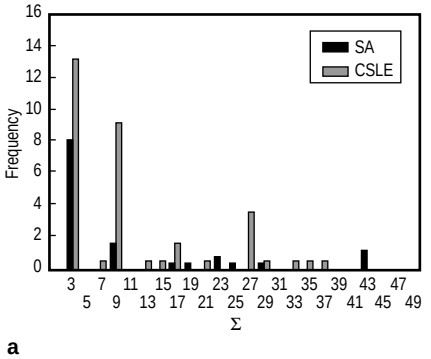

a

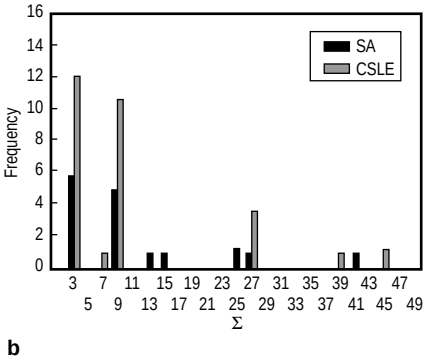

b

Figure 1. An example of the grain boundary character distribution in (a) coarse grain (330 μm) and (b) small grain (35 μm) SA and CSLE samples.

INTRODUCTION

A grain boundary can be classified geometrically in terms of the relative misorientation between the adjacent grains. This relative misorientation can be defined by misorientation axis and angle, with certain specific combinations resulting in the coincidence of lattice points from each grain's crystal lattice creating a coincidence-site lattice (CSL).[1] The degree of coincidence is represented by the reciprocal density of common lattice points, denoted as the Σ number (e.g., the grains adjacent at a Σ5 boundary have one-fifth of their representative crystal lattice points in coincidence). It has been shown that low-angle boundaries (LABs), which have misorientation angles of less than 15°, and coincident-site lattice boundaries (CSLBs) with low Σ orientation ($\Sigma \leq 49$) display improved physical and chemical properties relative to general or high-angle boundaries (HABs) ($\Sigma > 49$).[2–4] As compared with higher Σ boundaries, low Σ grain boundaries possess lower energy in pure metals;[5] less susceptibility to solute segregation;[6] lower diffusivity;[7] and greater resistance to sliding,[8] cavitation,[9] localized corrosion,[3] and fracture.[10]

Nickel-based alloy 600 has been used for pressurized-water-reactor (PWR) steam-generator tubing because of its general corrosion resistance as well as its resistance to localized attack in aqueous environments containing chloride. However, alloy 600 was found to be susceptible to intergranular stress corrosion cracking (IGSCC) on the primary side in the highly stressed areas of tubes (roll transition areas, inner-row U-bends)[11] and on the secondary side in the tube/tube-sheet region.[12] It is well known that IGSCC of alloy 600 is a manifestation of an essential interplay between stress, environment, and susceptible microstructure. Of these parameters, the microstructure has been the most difficult to define because of the high degree of variability.[13] Considerable efforts have also been made to correlate intergranular (IG) cracking with characteristics of the grain-boundary microstructure, including grain-boundary misorientation.[14–19] Aust et al.[15] have attempted to optimize microstructures of alloy 600 via alteration of the grain-boundary character distribution (GBCD), which describes the distribution of grain-boundary types in an alloy. They found that an increase in the CSLB content resulted in a reduced susceptibility of alloy 600 in the nonsensitized condition to intergranular attack. In addition, the corrosion rate after sensitization also diminished with an increasing fraction of CSLBs.

Although evidence indicates that the IGSCC susceptibility of alloy 600 can be reduced via alteration of the GBCD,[14–16] the connection between the role of the GBCD and mechanisms that are responsible for IGSCC susceptibility is not well understood. Recent research also indicates that the phenomenon of creep and the manner by which the grain boundary responds to creep deformation may play a significant role in the IGSCC susceptibility of Ni-16Cr-9Fe alloys.[20–21] Furthermore, the effect of the environment on increasing the amount of intergranular cracking of this alloy enhances the creep component.[22]

GRAIN BOUNDARY SYNTHESIS AND CHARACTERIZATION

Ultrahigh-purity Ni-16Cr-9Fe alloys were used in this study to eliminate complications from heat-to-heat variations in composition and other microstructural variables (e.g., impurity elements and/or second-phase particles). Feedstock alloys were electron-beam melted, and the melt was then cast and swaged down to a 3.05 mm rod from which tensile bars with a gage diameter of 2.2 mm were prepared. Samples in the solution-annealed (SA) and CSL-enhanced (CSLE) conditions were used with grain sizes of 35 μm and 330 μm. CSL enhancement was obtained through a sequence of deformation and annealing stages (usually two or three stages), where deformation consisted of tensile straining from 2–5% followed by annealing in the range of 890°C to 940°C for 1–20 hours.

Characterization of the resulting GBCDs was made using electron channeling pattern (ECP) analysis for large-grain samples[23] and electron backscattering pattern (EBSP) analysis for small-grain samples.[24] The fraction of grain boundaries classified as HABs, LABs, or CSLBs are shown in Figure 1 for samples of both grain sizes in both

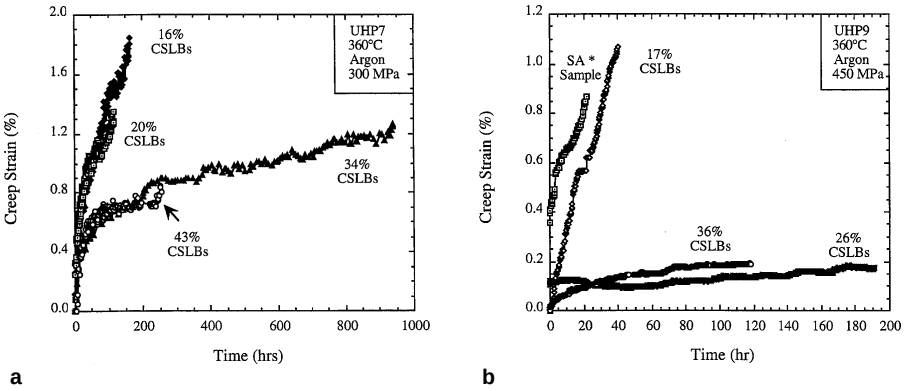

a b

Figure 2. Constant load creep curves of (a) coarse grain and (b) small grain SA and CSLE samples in 360°C argon at 300 MPa and 450 MPa, respectively.

the SA and CSLE conditions. Solution annealing generally resulted in 16–20% of the boundaries classified as LAB or CSL, while deformation and annealing sequences increased the percentage to 26–43%, about double the concentration. It should also be noted that these techniques were conducted manually, resulting in the analysis of many fewer boundaries than by automated systems. Coherent twins are excluded from this analysis, which results in a significantly lower fraction of Σ3 boundaries and, hence, a lower fraction of CSL boundaries.

GRAIN BOUNDARY CHARACTER DISTRIBUTION AND CREEP

Figure 2 shows constant-load creep curves of SA and CSLE samples of two different grain sizes in 360°C argon. The steady-state creep rate was found to decrease rapidly with increasing proportions of CSLBs, with the creep rate being reduced by a factor of 10–30 in the CSLE samples. Besides the difference in overall creep rate, another striking difference was in the distribution of creep strain between the creep regimes. In SA samples, primary creep accounted for the majority of the total creep life, while the CSLE samples spent the bulk of their creep life in the secondary creep stage.

Insight into the deformation process is provided by the stress dependence on creep. Figure 3 shows that the creep rate decreases with a decreasing applied stress, as expected; however, the creep rates for SA and CSLE samples are considerably different for the same stress. Extrapolating the creep rate to zero yields values for the magnitudes of the internal stress: 445 MPa for the CSLE sample and 415 MPa for the SA sample. (Since measurements are dependent on the resolution of the system, the "zero" creep rate becomes 5×10^{-10} s^{-1} for our system.) The internal stress is important because the rate of deformation is not driven by the applied stress but by the effective stress, which is the difference between the applied stress and the internal stress.[25] The magnitude of the internal stress reflects the state of the microstructure relevant to the deformation kinetics.

Another consequence of an increase in the CSLB fraction is an increase in the flow stress. Constant-extension-rate experiments conducted to 1.25% strain showed that the increased CSLB fraction correlates well with an increase in flow stress, as shown in Figure 4.

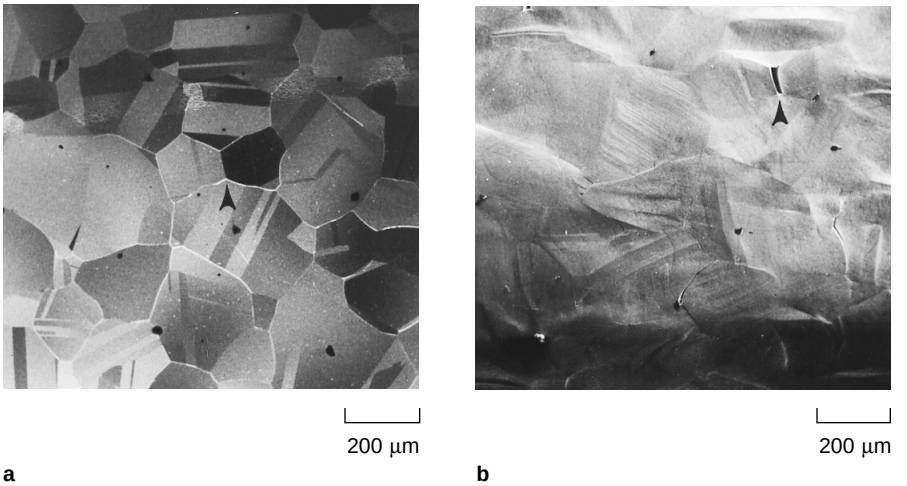

a b

Figure 5. (a) A backscatter electron image of a region on SA sample C7 before testing, and (b) a secondary electron image of the same region after constant extension rate testing in high-purity water at 360°C to 40 percent elongation. The arrows point to the same boundary in each micrograph.

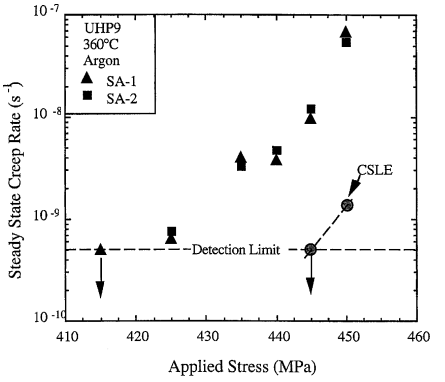

Figure 3. The dependence of the steady-state creep rate on applied stress for two small-grain SA samples and a CSLE sample in 360°C argon.

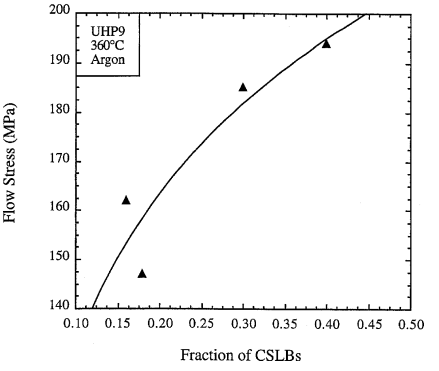

Figure 4. The dependence of flow stress on CSLB fraction after straining at a constant extension rate to 1.25% plastic strain in 360°C argon.

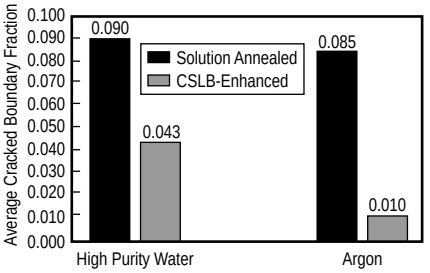

Figure 6. An average cracked boundary fraction for coarse-grain SA and CSLE samples after constant extension rate tests in 360°C high-purity water or argon.

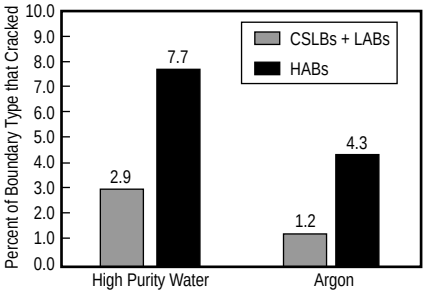

Figure 7. The percentage of total boundary types that cracked (coarse-grain SA and CSLE samples combined) after constant extension rate tests at 360°C in high-purity water or argon.

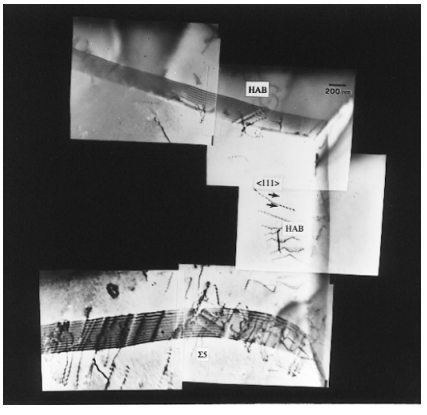

Figure 8. An example of EGBD density in random high-angle and CSL boundaries in an SA sample after 1.25% plastic strain in 360°C argon at a strain rate of 8×10^{-7} s^{-1}.

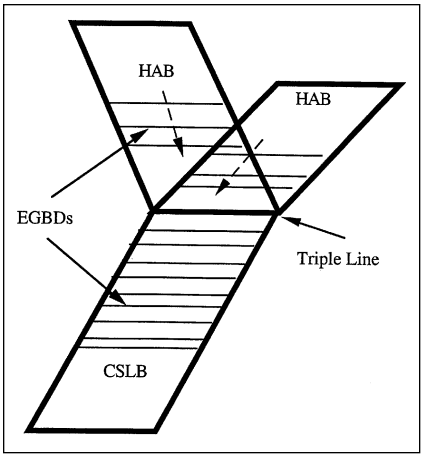

Figure 9. A schematic of dislocation annihilation at a triple line.

GRAIN BOUNDARY CHARACTER DISTRIBUTION AND INTERGRANULAR CRACKING

The effect of GBCD on the IGSCC and IG cracking behavior of pure Ni-16Cr-9Fe was assessed by determining if LABs or CSLBs are more crack resistant than GHABs in argon and deaerated high-purity water. The cracking susceptibility of boundary types was determined using constant-extension-rate tensile tests (CERTs) in 360°C argon and in deaerated high-purity water. CERTs in argon were performed to allow discrimination between behavior attributable to the water environment and behavior inherent in the mechanical deformation of the alloy. The susceptibility of grain-boundary types to IGC and IGSCC was quantified by determining the relative proportion of cracked boundaries by type and the cracked boundary fraction (i.e., the number of cracked boundaries on a sample surface divided by the estimated total number of boundaries on the surface) for each sample. These determinations were made using scanning electron microscopy images of samples surfaces after mechanical testing and by correlating observed cracked boundaries with boundary types determined prior to testing, as illustrated in Figure 5.

Evaluation of the cracked-boundary fractions for SA and CSLE samples tested in either environment indicated that, in general, CSLE samples exhibited less surface cracking than did SA samples (Figure 6). Because the cracked-boundary fractions allowed discrimination of the behavior of the two sample types, it is also apparent that a bulk behavior property (i.e., surface crack density) is a sufficient parameter for assessing the relative cracking susceptibility of samples with a two-fold difference in special boundary proportions.

Of the boundary types, LABs did not crack on any of the samples; this may be partially attributable to the fact that so few were present. CSLBs were more resistant to cracking in either environment for either type of sample. The percentage of each type of boundary that cracked is shown in Figure 7, where CSLBs and LABs were combined and the total of each grain-boundary type is plotted without regard to sample type (CSLE vs. SA). As shown, irrespective of environment, CSLBs and LABs crack significantly less than HABs.

While CSLBs are not immune to cracking in either environment, they are apparently more susceptible to cracking in deaerated high-purity water than in an inert atmosphere. This behavior is consistent with observations by Priester[7] that grain-boundary phenomena that are mechanical in nature depend on the misorientation between the grains adjacent at the boundary; other phenomena (e.g., grain-boundary diffusion or segregation) depend on the actual atomic structure at the boundary, inferences of which would require characterization of the grain boundary plane orientation as well. Because the CSL model classifies grain boundaries based only upon their relative misorientation across the boundary (i.e., three of the five degrees of freedom of a grain boundary), phenomena that depend on the orientation of the grain boundary plane as well are not likely to correlate with the CSL model. Therefore, the resistance of a CSLB to cracking in high-purity water may depend on phenomena influenced by the orientation of the grain boundary plane.

Although CSLE samples exhibited less surface cracking than SA samples, both types exhibited roughly the same amount of intergranular cracking or faceting on fracture surfaces (visually determined to be 13–23 percent of the fracture surface). This result, when considered with the observations described above, indicates that crack initiation on the surface is more sensitive to GBCD than crack propagation through the material, at least for the proportion of special boundaries considered. This result is not surprising when one considers that even the CSLE samples had more GHABs than CSLBs; therefore, a propagating crack would be more likely to encounter GHABs rather than the more crack-resistant CSLBs.

GRAIN BOUNDARY MISORIENTATION EFFECTS AND DEFORMATION

The increase in creep resistance and flow strength, coupled with the slower kinetics of dislocation annihilation at CSLBs, provides the link between GBCD and creep deformation. It is hypothesized that an increase in the CSLB population in the system decreases the annihilation rate of dislocations in the grain boundary, leading to an increase in the internal stress and a decrease in the effective stress. The result is a reduction in the creep strain rate.

It is envisioned that the absorption of a lattice dislocation into a CSL boundary is a difficult process due to the highly ordered structure. Therefore, subsequent lattice dislocations approaching the CSLB during deformation will be opposed by the first dislocations trapped there.[26] A long-range internal stress thus arises due to the stress field of leading dislocations, which then inhibits the motion of following dislocations. On the contrary, the process of dislocation absorption in HABs can be considered as equivalent to the total annihilation of dislocations, which relaxes the boundaries and results in the disappearance of long-range strain fields.[27] Hence, the rate of formation and absorption of extrinsic grain boundary dislocations (EGBDs), created when a lattice dislocation interacts with a grain boundary during plastic deformation, is of

practical importance since it may be related to the rate at which backstresses on the following dislocations are relaxed, and this relaxation may control the rate of deformation.[28] As such, samples with differences in absorption kinetics (i.e., CSLB fraction) may then relax at different rates leading to differences in the internal stress. The concept of a difference in absorption kinetics translating into a higher internal stress may be viewed in accordance with the widely accepted idea that creep deformation of crystalline solids at high temperatures does not take place under the action of the whole applied stress but only under a part of it.

Using transmission electron microscopy images, measurements were made of the density of EGBDs in HABs and CSLBs to determine the relative ease of incorporation of run-in lattice dislocations into each boundary type. In order to minimize the question of heterogeneity due to small plastic deformation, comparisons of EGBD density between grain boundary type were carefully chosen on adjacent boundaries that bordered the same grain. The mean EGBD density for each grain boundary type was calculated with a 95% confidence interval using a student-t distribution; in every case, the EGBD density in CSLBs was found to be approximately three times higher than that in HABs, regardless of the thermo-mechanical history of the samples and Bragg reflection conditions.

This difference is shown in the TEM micrograph of Figure 8, in which the EGBD density is observed to be significantly higher in the Σ5 boundary versus the HABs. As the average EGBD density of CSLBs is approximately three times higher than that of HABs for both types of samples, it is apparent that an HAB can absorb more lattice dislocations per unit strain than a CSLB. This conclusion is consistent with those of several authors whose works have qualitatively shown a large difference in the absorption rate between coincidence and random high-angle boundaries.[29–32] The absorption process has generally been described as dissociation of run-in lattice dislocations into displacement-shift complete (DSC) dislocations followed by their separation in the boundary plane under the influence of forces of mutual repulsion.[33] As the grain boundary becomes less ordered, the DSC vectors are smaller and the dissociation reaction becomes more energetically favorable, thus making the absorption of lattice dislocations easier.

The role of CSLBs in creep deformation is to increase the internal stress by trapping run-in lattice dislocations at the grain boundaries and creating backstresses on the following dislocations rather than annihilating them, as in the case of HABs. This view is consistent with measurements that show a difference in the internal stress of approximately 30 MPa between CSLE and SA conditions. It is thus concluded that the lower dislocation absorption kinetics and the higher internal stress of a CSLE sample are responsible for the lower creep rate. To further substantiate the suggested explanation for the effect of the CSLB fraction on creep rate, we need to be able to quantitatively explain its dependence on the CSLB fraction.

At steady state, the creep rate is a balance between dislocation generation and annihilation. Transmission electron microscopy results revealed a large difference in the absorption rate between CSLBs and HABs, indicating that the rate of dislocation annihilation at grain boundaries must be different between CSLE and SA samples. Based on Sangal and Tangri's model[34] for the annihilation of extrinsic grain boundary dislocations at triple lines (i.e., junctions of three grain boundaries), it is proposed that EGBD annihilation at triple lines can only occur if at least two of the intersecting grain boundaries are HABs, since only EGBDs on HABs can climb to the triple lines (Figure 9).[35] On the basis of geometric considerations, we can define the probability of EGBDs annihilating at a triple line by calculating the probability of finding at least two high-angle boundaries at a triple line, P_{TL}, which is given by

$$P_{TL} = (1 - f_{CSLB})^3 + (f_{CSLB})(1 - f_{CSLB})^2 = (1 - f_{CSLB})^2 \quad (1)$$

where f_{CSLB} is the fraction of boundaries in the sample that are classified as CSLBs. The first term in Equation 1 represents the probability of finding all three high-angle boundaries at a triple line, and the latter term represents the probability of finding two high-angle boundaries and one CSLB at a triple line. Since there are n number of triple lines per grain (Figure 10), the probability that all of the triple lines surrounding a grain are operative as annihilation sites, ξ, can be expressed as

$$\xi = P_{TL}^{n} \quad (2)$$

As such, the expression for the steady-state creep rate should include the quantity ξ to account for that portion of the grain boundary volume that is acting as an annihilation site. The creep rate is written as

$$\dot{\varepsilon} = A\xi V_{GB} \dot{\rho}_a^- \Big|_{GB} \quad (3)$$

where A is a constant that is proportional to the Burgers vector, and the average dislocation spacing, V_{GB}, is the grain boundary volume. $\dot{\rho}_a^- \Big|_{GB}$ is the rate of dislocation annihilation at grain boundaries, and the term ξ is an indicator of the "effective" grain boundary volume fraction taking part in the annihilation process. The ratio of the steady-state creep rate between the SA and the CSLE sample at steady state can thus be expressed as

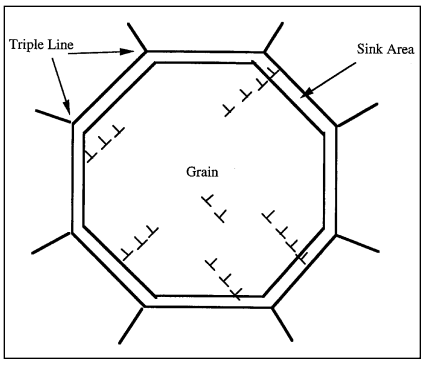

Figure 10. A schematic of n number of triple lines per grain acting as dislocation annihilation sites.

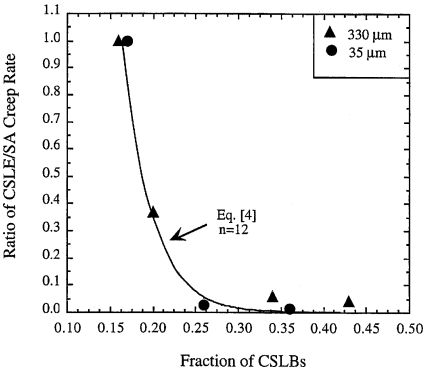

Figure 11. A comparison of measured and calculated ratios (Equation 4) of CSLE/SA creep rate with the CSLB fraction in coarse- and small-grain samples crept at 300 MPa and 450 MPa, respectively.

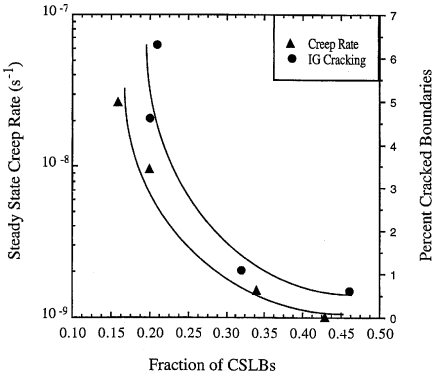

Figure 12. The dependence of steady-state creep rate and the percent of cracked boundaries on the CSLB fraction on coarse grain Ni-16Cr-9Fe in 360°C argon.

$$\frac{\dot{\varepsilon}^{CSLE}}{\dot{\varepsilon}^{SA}} = \frac{\xi^{CSLE}}{\xi^{SA}} = \frac{(P_{TL}^{n})^{CSLE}}{(P_{TL}^{n})^{SA}} = \frac{\left[\left(1-f_{CSLB}\right)^{2n}\right]^{CSLE}}{\left[\left(1-f_{CSLB}\right)^{2n}\right]^{SA}} \quad (4)$$

where superscripts SA and CSLE refer to the sample type.

Equation 4 was evaluated by using the previously determined fraction of CSLBs; the number of triple lines per grain, n, was chosen to be 12, which is the number of triple lines per grain of a tetrakaidecahedron representing the average topological form of grains in polycrystals.[36] To compare model predictions and measurements, the measured and predicted creep-rate ratio was plotted as a function of CSLB fraction for both 330 μm and 35 μm grain samples in Figure 11. From this figure, it is clear that this simple geometric model provides a good prediction of the nonlinear dependence of the steady-state creep rate ratio with CSLB fraction.

It should also be pointed out that in addition to being the primary sinks, grain boundaries may well be the primary sources for dislocations.[37] Although this study does not provide any evidence to indicate that grain boundaries are the primary sources for dislocations, it has been shown that dislocations are more easily emitted from HABs than CSLBs. In-situ transmission electron microscopy observations performed on stainless steel by Kurzydlowski et al.[38] confirmed that the generation of dislocations on a CSLB, Σ9, occurs at a shear stress 40 times higher than on the adjoining HAB. Thus, a HAB is a more efficient dislocation source than a CSLB. Regardless of whether grain boundaries act as primary sinks or sources for dislocations, an increase in the CSLB fraction should result in a reduction in the creep rate, since not only the rate of dislocation annihilation is decreased but also possibly the rate of dislocation generation.

One other mechanism that has not yet been addressed is the influence of EGBD movement on grain boundary sliding. Although grain boundary sliding is generally one of the important deformation mechanisms at high temperature, and although it is sensitive to grain boundary type,[39] it has previously been shown in this system[40] that grain boundary sliding accounts for no more than 2% of the total creep deformation. As a result, its contribution to the difference in creep deformation of CSLE and SA is not significant and need not be addressed by the model. The simple model considered here does not exhaust all the possible mechanisms by which lattice dislocations interact with grain boundaries, but it does account for the strong nonlinear dependence of creep rate on the CSLB fraction, using a known mechanism for dislocation annihilation.

THE RELATIONSHIP BETWEEN CREEP AND CRACKING

Results from creep in Ni-16Cr-9Fe samples in 360°C argon revealed that the steady-state creep rate was significantly reduced when the proportion of CSLBs was increased. In light of previous work,[22,41] it was demonstrated that the presence of a mechanical creep component greatly influences the IGSCC susceptibility. CERT experiments[14] on coarse-grain Ni-16Cr-9Fe in 360°C argon also showed that cracking susceptibility decreases with increasing proportions of CSLBs. Thus, it is not surprising that the increase in the fraction of CSLBs increases creep resistance and reduces cracking in the coarse-grain Ni-16Cr-9Fe alloys. To illustrate this statement, the steady-state creep rate and the percent of cracked boundaries of coarse-grain samples were plotted together with the fraction of CSLBs (Figure 12). From this, it is clear that the creep rate and the amount of intergranular cracking correlate with the CSLB fraction; the creep rate and the IG cracking decrease rapidly with an increasing fraction of CSLBs. Furthermore, the manner by which both creep and IG cracking correlates with the CSLB fraction may imply that creep and IG cracking are intimately linked. Because the macroscopic creep rate also reflects the rate of deformation at or near grain boundaries, the benefit of greater proportions of CSLBs in reducing cracking might be explained by considering the response of the grain boundary to creep deformation (i.e., grain boundary sliding and cavitation).

Investigation of grain boundary cavitation of the 330 μm grain creep samples[40] revealed that HABs were found to be preferentially cavitated relative to the CSL boundaries. However, it was also observed that all of the cavitated boundaries in the Ni-16Cr-9Fe sample also showed sliding, suggesting that grain boundary sliding is a precursor to cavitation. This eventually leads to intergranular cracking of Ni-16Cr-9Fe samples, although sliding does not account for much of the overall creep strain. This is important because it suggests that the operating mechanism responsible for intergranular cracking in Ni-16Cr-9Fe at 360°C may be controlled by grain boundary sliding rather than slip-induced cavitation. Our results are consistent and support the idea that the role of CLSBs in reducing dislocation annihilation kinetics accounts for both a reduction in creep rate and a reduction in the amount of IGSCC in high-purity Ni-16Cr-9Fe at high temperature.

Watanabe[39] has previously demonstrated that the amount of sliding strongly depends on the type and misorientation of grain boundaries and occurs more easily on HABs. Although the sliding mechanism is still a matter of dispute, it has been accepted

References

1. A.P. Sutton, *Int. Met. Rev.*, 29 (1984), pp. 377–402.
2. L.S. Shvindlerman and B.B. Straumal, *Acta Metall.*, 33 (1985), pp. 1735–1749.
3. G. Palumbo et al., *Mater. Res. Soc. Symp. Proc.*, 238 (Pittsburgh, PA: MRS, 1992), p. 311.
4. K.T. Aust, U. Erb, and G. Palumbo, *Mechanical Properties and Deformation Behavior of Materials Having Ultra-Fine Microstructure*, NATO ASI Series (Netherlands: Kluwer, 1993), p. 107.
5. P.J. Goodhew, *Metal Sci. J.*, 13 (1979), pp. 108–117.
6. D. Bouchet and L. Priester, *Scripta Metall.*, 21 (1987), pp. 475–478.
7. L. Priester, *Revue Phys. Appl.*, 21 (1989), pp. 419–438.
8. H. Kokawa, T. Watanabe, and S. Karashima, *Phil. Mag. A*, 40 (1981), pp. 1239–1254.
9. J. Don and S. Majumdar, *Acta Metall.*, 34 (1986), pp. 961–967.
10. T. Watanabe, *J. de Physique*, 5 (1988), pp. 507–519.
11. K. Norring and J. Engstrom, *1985 Workshop on Primary-Side Stress Corrosion Cracking of PWR Steam Generator Tubing*, NP-5158, ed. A.R. McIlree (Palo Alto, CA: EPRI, 1987), paper 3.
12. A.K. Agrawal and G. Frieling, *1987 Workshop on Secondary-Side Intergranular Corrosion Mechanisms*, NP-4458 (Palo Alto, CA: EPRI, 1988).
13. G.P. Airey, *Third International Symposium on Environmental Degradation of Materials in Nuclear Power Systems-Water Reactors* (Houston, TX: NACE, 1984), pp. 462–478.
14. D.C. Crawford and G.S. Was, *Metall. Trans. A*, 23, (1992), pp. 1195–1206.
15. K.T. Aust, U. Erb, and G. Palumbo, *Mat. Sci. Eng.*, A176 (1994), pp. 329–334.
16. P. Lin et al., *Scripta Metall. et Mat.*, 33 (1995), pp. 1387–1392.
17. E.M. Lehockey et al., *Scripta Mat.*, 36 (1997), pp. 1211–1218.
18. G. Palumbo, E.M. Lehockey, and P. Lin, *JOM*, 50 (2) (1998), pp. 40–43.
19. V. Randle, *JOM*, 50 (2) (1998), pp. 56–59.
20. G.S. Was, J.K. Sung, and T.M. Angeliu, *Metall. Trans.*, 23A (1992), pp. 3343–3359.
21. G.S. Was, T.M. Angeliu, and J.K. Sung (paper presented at the Alloy 600 Experts Meeting, Warrenton, VA, 6–9 April, 1993).
22. T.M. Angeliu, Ph.D. thesis, University of Michigan (1993).
23. D.C. Crawford and G.S. Was, *J. Electron Microcopy Technique*, 19 (1991), pp. 345–360.
24. V. Thaveeprungsriporn, J.F. Mansfield, and G.S. Was, *J. Mater. Res.*, 9 (7) (1994), pp. 1887–1894.
25. J. Cadek, *Mat. Sci. Eng.*, 94 (1987), pp. 79–92.
26. D.J. Dingley and R.C. Pond, *Acta Metall.*, 27 (1979), pp. 667–682.
27. W. Lojkowski, *Acta Metall. et Mater.*, 39, 8 (1991), pp. 1891–1899.
28. A.H. King, *Scripta Metall.*, 19 (1985), pp. 1517–1521.
29. H. Kokawa, T. Watanabe, and S. Karashima, *Phil. Mag. A*, 44 (6) (1981), pp. 1239–1254.
30. H. Kokawa, T. Watanabe, and S. Karashima, *J. of Mater. Sci.*, 18 (1983), pp. 1183–1194.
31. T. Johannesson and A. Thölén, *Metal Sci. J.*, 6 (1972), p. 189.
32. P.R. Howell, J.O. Nilsson, and G.L. Dunlop, *Phil. Mag. A.*, 38 (1) (1978), pp. 39–47.
33. W.A.T. Clark and D.A. Smith, *J. of Mater. Sci.*, 14 (1979), p. 776.
34. S. Sangal and K. Tangri, *Metall. Trans. A*, 20 (1989), p. 479–486.
35. V. Thaveeprungsriporn and G.S. Was, *Metall. Trans. A*, 28A (1997), pp. 2101–2112.
36. F.N. Rhines, K.R. Craig, and R.T. DeHoff, *Metall. Trans.*, 5 (1974), pp. 413–425.
37. L.E. Murr and S.H. Wang, *Res Mechanica*, 4 (1982), pp. 237–274.
38. K.J. Kurzydlowski, R.A. Varin, and W. Zielinski, *Acta Metall.*, 32 (1984), pp. 71–78.
39. T. Watanabe, *Metall. Trans. A*, 14A (1983), pp. 531–545.
40. V. Thaveeprungsriporn et al., *Sixth International Symposium on Environmental Degredation of Materials in Nuclear Power Systems-Water Reactors* (Warrendale, PA: TMS, 1993), pp. 721–727.
41. J.K. Sung and G.S. Was, *Corrosion*, 47 (1991) p. 824.
42. H. Kokawa, T. Watanabe, and S. Karashima, *Phil. Mag. A*, 40 (1981), pp. 1239–1254.
43. R.C. Pond, D.A. Smith, and P.W.J. Southerden, *Phil. Mag. A*, 37 (1978), pp. 27–40.
44. L.C. Lim and R. Raj, *Acta Metall.*, 32 (1984), pp. 1183–1190.
45. L.C. Lim and R.J. Raj, *J. de Phys.*, supplement no. 4, 46 (1985), pp. c4-581–c4-595.
46. T.C. Lee, I.M. Robertson, and H.K. Birnbaum, *Scripta. Metall.*, 23 (1989), pp. 799–803.

that the process must involve the absorption of lattice dislocations into the grain boundary[42] and movements of dislocations along the grain boundary plane.[43] Thus, a lattice dislocation impinging upon an HAB can be easily absorbed and dissociated into grain boundary structural dislocations with small Burgers vectors, which can then glide and climb along the grain boundary plane, resulting in grain boundary sliding. Conversely, a lattice dislocation tends to be retained as an EGBD in the CSLB since absorption and dissociation is more difficult. As a result, the CSLB will exhibit less sliding as compared with the HAB. This view is consistent with the results revealing that the average EGBD density in CSLBs is approximately three times higher than that in HABs. It is apparent that an HAB can absorb more lattice dislocations per unit strain than a CSLB.

CSLBs are not only resistant to sliding, but also to high-temperature fracture and cavitation. Lim and Raj[44] also demonstrated that the high Σ boundaries are the first to cavitate in low-cycle fatigue tests of nickel. However, with increasing applied strain, the low Σ boundaries (Σ3 and Σ9) eventually develop cavities. They proposed a model to explain the formation of slip-induced cavities in nickel that incorporates the ability of a CSLB to re-emit dislocations. According to their model, HABs and higher Σ CSLBs would dissociate absorbed lattice dislocations into grain boundary dislocations with smaller Burgers vectors less able to induce slip in adjoining grains. Further, the more a boundary deviates from an exact coincidence orientation, the more likely it is to accumulate residual grain boundary dislocations,[45,46] leading to an accumulation of strain energy. Accordingly, these boundaries would be more apt to reduce their strain energy by cavitating. However, our results do not provide sufficient evidence to evaluate the role that slip transmission and inducement might have in the observed IG cracking results. Nevertheless, it is instructive to note that the model proposed for creep deformation exhibited excellent agreement without consideration of these other phenomena, and that grain boundary sliding dependence can be explained using a similar mechanism.

CONCLUSION

Evidence supports a model for a reduction in creep rate and IGSCC by the interaction of dislocations with CSLBs. The increased difficulty of incorporating matrix dislocations into CSLBs vs. HABs gives rise to an increase in the internal stress by trapping run-in lattice dislocations at the grain boundaries and creating backstresses on the following dislocations. The net result is a reduction in the dislocation annihilation rate and a corresponding increase in the creep rate. Given that EGBD annihilation can occur at triple lines only if at least two of the intersecting grain boundaries are HABs, then annihilation and creep depends nonlinearly on the fraction of CSLBs in the solid. The effect of CSLBs on creep extends as well to IGSCC in this alloy, in that both creep and IGSCC have the same dependence on CSLB fraction. This should not be surprising since it has been shown that the strain-rate dependence of IGSCC in high-purity Ni-16Cr-9Fe is due to creep. In fact, grain boundary cavitation, which has been shown to be the failure mode in high-purity Ni-16Cr-9Fe, is suppressed on CSLBs, resulting in a reduction in the amount of IGSCC. Hence, the role of CLSBs in reducing dislocation annihilation kinetics accounts for a reduction in the creep rate and can conceivably account for a reduction in the amount of IGSCC in high-purity Ni-16Cr-9Fe at high temperature.

ACKNOWLEDGEMENTS

The authors gratefully acknowledge facilities provided by the High Temperature Corrosion Laboratory and the Electron Microbeam Analysis Laboratory at the University of Michigan. This work was supported by the Office of Basic Energy Sciences of the U.S. Department of Energy under grant number DE-FG02-85ER45184.

ABOUT THE AUTHORS

Gary S. Was earned his Sc.D. in nuclear materials at the Massachusetts Institute of Technology in 1980. He is currently a professor and chair of the Department of of Nuclear Engineering and Radiological Sciences at University of Michigan. Dr. Was is a member of TMS.

Visit Thaveeprungsiporn earned his Ph.D. in nuclear engineering at the University of Michigan in 1966. He is currently a lecturer in the Department of Nuclear Technology, Faculty of Engineering at Chulalongkorn University, Thailand. Dr. Thaveeprungsiporn is also a member of TMS.

Douglas C. Crawford earned his Ph.D. in nuclear engineering at the University of Michigan in 1991. He is currently department manager of fuels technology in the Engineering Division at Argonne National Laboratory.

For more information, contact Gary S. Was, 1911 Cooley Building, 2355 Bonisteel Boulevard, Ann Arbor, Michigan 48109; (734) 763-4675; fax (734) 763-4540; e-mail gsw@umich.edu.